Network Entropy Analysis using the Maxwell-Boltzmann Partition Function

Jianjia Wang, Richard C. Wilson, Edwin R. Hancock
Department of Computer Science,
Computer Vision and Pattern Recognition,
University of York, York, YO10 5DD, UK
Email: {jw1157, Richard.Wilson, Edwin.Hancock}@york.ac.uk

***Abstract*—In this paper, we use the Maxwell-Boltzmann partition function to compute network entropy. The partition function is used to model the energy level population statistics where the network is in thermodynamic equilibrium with a heat-bath. Here the network Hamiltonian operator defines a set of energy levels occupied by particles in thermal equilibrium. These energy levels are given by the eigenvalues of the normalized Laplacian matrix. In other words, we investigate a thermalised version of the system normally studied in spectral graph theory, where the thermalisation accounts for noise in the system. We provide a systematic study of the entropy resulting from this characterization. Compared to previous work based on using von Neumann network entropy, this thermodynamic quantity is effective in characterizing changes of network structure and distinguishing different types of network models (e.g. Erdős-Rényi random graphs, small world networks, and scale free networks). Numerical experiments on real world data-sets are presented to evaluate the qualitative and quantitative differences in performance.**

1. Introduction

There has been a considerable amount of work aimed at developing effective characterizations of complex network structure. Broadly speaking, two approaches have been used to solve the problem of characterizing variations in network structure and evolution over time. The first approach is based on the application of graph-spectral techniques, while the second is to capture uncertainties using statistics or probability [1], [2], [3]. Most of the available characterizations have centred around ways of capturing network substructure using clusters, hubs and communities [1], [2], [3]. The underlying representations are usually based on simple degree statistics which capture the network connectivity structure [4], [5]. Although these available methods are goal directed, one potentially promising approach is to draw on ideas from classical and quantum statistical physical models of network systems.

For instance, the Boltzmann distribution from classical statistical mechanics has been used to quantify network properties [1], [3]. This method maximizes the ensemble entropy in exponential random graphs to predict their time-evolution [3]. Physical models from statistical mechanics can also provide robust tools for characterizing the differences between different classes of complex network structures [2]. Using a heat reservoir analogy from thermodynamics, microscopic measures of communicability and balance in networks can be defined [1]. Although these physical analogies are useful, there is no easy way to link directly the physically-based statistical mechanics to the graph spectral representation of networks.

On the other hand, a thermodynamic analogy based on the heat bath provides a convenient route to derive network characterizations from the physical properties. The energy states can be generated if the Hamiltonian operator is equated with a suitably defined matrix representation of the network. In this case the eigenvalues of the matrix are the energy eigenvalues. In the heat-bath analogy these energy states are populated by particles subject to thermal equilibrium. The network reaches thermal equilibrium with the heat bath, and this determines how many particles occupy at each state. If the particles behave in a classical way, i.e. they are distinguishable, then as a result of this thermalisation, these particles will occupy at the Laplacian eigenstates according to the Boltzmann distribution [1], [6].

Formally, a partition function for this type of system is helpful, since it provides a computational link between the microscopic properties of the energy states and the macroscopic properties of the network. To compute the partition function requires a Hamiltonian operator for the network. Usually, the network Hamiltonian derives from the adjacency or Laplacian matrix of the network, but recently, Ye et al. [6], have shown how the partition function can be computed from a characteristic polynomial instead.

Furthermore, the partition function provides a natural starting point in describing the network statistics and evolution, from which thermodynamic characterizations of the network can then be derived [6], [8]. By specifying the microstates of the network system, statistical characterizations can succinctly provide deep insights into network behavior. In this paper, we use the Maxwell-Boltzmann partition function to describe the thermalisation of the normalized Laplacian eigenstates of the network. From this model we compute global network characteristics, including the entropy, from the graph spectra.

2. Graph Representation

Let $G(V, E)$ be an undirected graph with node set V and edge set $E \subseteq V \times V$, and let $N = |V|$ represent the total number of nodes on graph $G(V, E)$. The adjacency matrix A

Preprint submitted to 23rd International Conference on Pattern Recognition.
Received April 19, 2016.

of a graph is defined as

$$A = \begin{cases} 0 & \text{if } (u,v) \in E \\ 1 & \text{otherwise.} \end{cases} \tag{1}$$

Then the degree of node u is $d_u = \sum_{v \in V} A_{uv}$. The Laplacian matrix of a graph G is $L = D - A$ and D denotes the degree diagonal matrix whose elements are given by $D(u,u) = d_u$ and zeros elsewhere.

The normalized Laplacian matrix $\tilde{L}$ is defined as

$$\tilde{L} = D^{-\frac{1}{2}} L D^{\frac{1}{2}} \tag{2}$$

where the element-wise expression of $\tilde{L}$ is

$$\tilde{L}_{uv} = \begin{cases} 1 & \text{if } u = v \text{ and } d_u \neq 0 \\ -\frac{1}{\sqrt{d_u d_v}} & \text{if } u \neq v \text{ and } (u,v) \in E \\ 0 & \text{otherwise.} \end{cases} \tag{3}$$

2.1. Hamiltonian Operator of a Graph

In quantum mechanics, the Hamiltonian operator is the sum of the kinetic energy and potential energy of all the particles in the system. It describes the particle propagate according to the Schrödinger equation. The Hamiltonian is given by

$$\hat{H} = -\nabla^2 + U(r,t) \tag{4}$$

There are number of ways to define the Hamiltonian operator of a graph. If the eigenvalues of graph with the Laplacian matrix can be viewed as the energy eigenstates, we then take the kinetic energy operator $-\nabla^2$ to be the negative of the normalized adjacency matrix, i.e. $-\tilde{A}$, and the potential energy $U(r,t)$ to be the identity matrix I. The Hamiltonian operator is viewed as the normalized form of Laplacian matrix on graph.

$$\hat{H} = I - \tilde{A} = \tilde{L} \tag{5}$$

2.2. Network Thermodynamic Representation

A network can be viewed as a canonical ensemble, which exchanges energy with a heat reservoir. The underpinning idea is that statistical thermodynamics can be combined with network theory to characterize both static and dynamic networks [8]. In general the energy and entropy of the network depend on the assumptions concerning the Hamiltonian and the corresponding partition function.

Here we consider the network as a thermodynamic system specified by particles with the energy states given by the Hamiltonian operator. The network is immersed in a heat bath with temperature parameter T. Then the partition function $Z(\beta, N)$ can be used to represent the network ensemble, where $\beta = 1/k_B T$ and k_B is the Boltzmann constant. The thermodynamics variables can be computed from the partition function. Specified in this way, we briefly review various thermodynamic characterizations of the network, i.e. Helmholtz free energy, entropy, average energy, associated with partition function.

The average energy of the network can be expressed in terms of the Hamiltonian operator,

$$U = \langle H \rangle = k_B T^2 \left[\frac{\partial}{\partial T} \log Z \right]_N = \left[-\frac{\partial}{\partial \beta} \log Z \right]_N \tag{6}$$

Then, the Helmholtz free energy is given by

$$F(\beta, N) = -\frac{1}{\beta} \log Z(\beta, N) = -k_B T \log Z(\beta, N) \tag{7}$$

and the thermodynamic entropy by

$$S = k_B \left[\frac{\partial}{\partial T} T \log Z \right]_N = k_B \left[\log Z + \beta \langle U \rangle \right]_N \tag{8}$$

The Helmholtz free energy may thus also be expressed in terms of the average particle energy $\langle U \rangle$, together with the entropy S and temperature T

$$F = \langle U \rangle - TS \tag{9}$$

As a result the temperature is given by

$$T = \left(\frac{\partial U}{\partial S} \right)_N = \frac{1}{k_B \beta} \tag{10}$$

2.3. Maxwell-Boltzmann Statistics

In statistical mechanics, the Maxwell-Boltzmann distribution relates the thermodynamic properties of particles from the microscopic perspective [13]. It applies to systems consisting of a fixed number of weakly interacting distinguishable particles. These particles occupy the energy states associated with a Hamiltonian [3].

Taking the Hamiltonian of the network to be the normalized Laplacian matrix, for Maxwell-Boltzmann occupation statistics in energy states, the canonical partition function is

$$Z_{MB} = \mathrm{Tr}\left[\exp(\tilde{L})^N \right] = \left(\sum_{i=1}^{V} e^{\beta \varepsilon_i} \right)^N \tag{11}$$

where $\beta = 1/k_B T$ is the reciprocal of the temperature T with k_B as the Boltzmann constant; N is the total number of particles and ε_i denotes the microscopic energy of system at each microstate i.

Furthermore, derived from Eq.(6), the average energy of the network is

$$\begin{aligned} \langle U \rangle_{MB} &= -\frac{\partial \log Z}{\partial \beta} \\ &= N \frac{\mathrm{Tr}[\tilde{L} \exp(-\beta \tilde{L})]}{\mathrm{Tr}[\exp(-\beta \tilde{L})]} = N \frac{\sum_{i=1}^{V} \varepsilon_i e^{-\beta \varepsilon_i}}{\sum_{i=1}^{V} e^{-\beta \varepsilon_i}} \end{aligned} \tag{12}$$

and similarly from Eq.(8), the corresponding entropy of the system with N particles is

$$\begin{aligned} S_{MB} &= \log Z - \beta \frac{\partial \log Z}{\partial \beta} \\ &= -N \frac{\mathrm{Tr}\left\{ \exp(-\beta \tilde{L}) \log[\exp(-\beta \tilde{L})] \right\}}{\mathrm{Tr}[\exp(-\beta \tilde{L})]} \\ &= -N \sum_{i=1}^{V} \frac{e^{-\beta \varepsilon_i}}{\sum_{i=1}^{V} e^{-\beta \varepsilon_i}} \log \frac{e^{-\beta \varepsilon_i}}{\sum_{i=1}^{V} e^{-\beta \varepsilon_i}} \end{aligned} \tag{13}$$

Preprint submitted to 23rd International Conference on Pattern Recognition.
Received April 19, 2016.

3. Experiments and Evaluations

We now explore whether the thermodynamic characterizations derived from the Maxwell-Boltzmann distribution, and in particular the entropy, can be employed as a useful tool for better understanding the structural properties of networks.

We commence by generating Erdős-Rényi random graphs, small world networks, and scale free networks, which represent the most three widely used models of network structure. Then, we turn our attention to a number of real world time-evolving networks to detect abrupt changes in network structure at different time epochs. Finally, this entropy method is applied to tumor mutation networks in order to distinguish the network structures corresponding to various types of cancers. To simplify the calculations, we fix the number of particle and set the Boltzmann constant to unity.

3.1. Data Sets

Here, we show three different data sets: the first one is synthetically generated artificial networks, while the remaining are extracted from real-world complex systems.

Data set 1: It contains 90 graphs which are randomly generated according to one of three different complex network models, namely, a) the classical Erdős-Rényi random graph model, b) the small-world model introduced by Watts and Strogatz [5], and c) the scale-free model developed by Barabási-Albert [14]. These are created using a variety of model parameters with graph size between 100 to 1,000. For small world networks, they are generated from Watts-Strogatz model [5] with rewiring probability $p = 0.2$ and average node degree $n = 20$. The scale free networks are derived from Barabási-Albert model [14] with preferential attachment $m = 10$ at each growing step.

Data set 2: The NYSE stock market database consists of daily prices of 3,799 stocks traded on the New York Stock Exchange [15]. A bunch of 347 stocks is selected from this data set, which contains the historical stock price from January 1986 to February 2011. The correlation based network is employed to represent the structure of the stock market. The time window of 20 days is applied to compute the cross correlation coefficients between the time-series for each pair of stock. Then the connections are created with a threshold $\xi = 0.85$.

Data set 3: The tumor mutation data contains three major cancers cataloged in the Cancer Genome Atlas (TCGA), namely a) ovarian, b) uterine and c) lung adenocarcinoma [16]. There are 356 patients with mutations in 9,850 genes for the TCGA ovarian cohort, 248 patients with mutations in 17,968 genes for the TCGA uterine endometrial cohort and 381 patients with mutations in 15,967 genes in the TCGA lung adenocarcinoma cohort [18]. Patient mutation networks were mapped onto gene interaction networks from PathwayCommons, which aggregates interactions from several pathway and interaction databases, focused primarily on physical protein-protein interactions (PPIs) and functional relationships between genes in canonical regulatory, signaling and metabolic pathways [17].

3.2. Simulation Results

We first investigate the thermodynamic entropy of artificial networks generated from three widely used models of complex network, namely the Erdős-Rényi random graph, the small-world Watts-Strogatz model [5] and the scale-free Barabási-Albert model [14]. These models provide a basis for analysing the statistical properties of different classes of complex networks. Here, we conduct numerical experiments to evaluate whether the Maxwell-Boltzmann entropy can distinguish differences in the structure and topology in different classes of the synthetic networks.

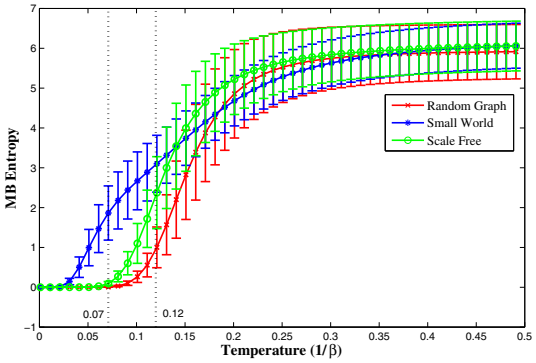

Figure 1. Maxwell-Boltzmann versus temperature. The red line represents Erdős-Rényi random graphs, the blue line small-world networks and the green line scale-free networks.

Fig.1 shows the average Maxwell-Boltzmann entropy and its standard deviation versus temperature for the three different classes of networks. The common feature is that for all three models the entropy increases monotonically with the temperature. At high temperatures, it is hard to distinguish different network structures. But at the temperature range between 0.07 to 0.12, the Maxwell-Boltzmann entropy clearly separates these three network models.

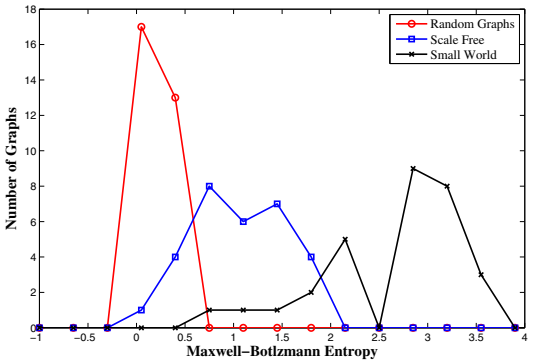

Figure 2. Histograms of Maxwell-Boltzmann entropy for three different synthetic networks. Each size of graph is randomly generated between $100 \sim 1000$ with temperature $\beta = 10$.

In order to better visualise these data, in Fig.2, we show histograms of Maxwell-Boltzmann entropy for data generated from the three different network models. The differently colored histogram represent the different network structures

Preprint submitted to 23rd International Conference on Pattern Recognition.
Received April 19, 2016.

(Erdős-Rényi, Watts-Stogatz and Barabási-Albert). It is clear that the Maxwell-Boltzmann entropy gives a good separation for the three kinds of network models.

Here, the experiments in this section show that the Maxwell-Boltzmann entropy can be efficiently used to distinguish different synthetic artificial networks. The main reason is that it captures differences in structural features of the distinct networks.

3.3. Experimental Results

Now we turn our attention to real-world networks, with the aim of establishing whether the Maxwell-Boltzmann entropy can be used to characterize the changes of network structures in time series and also distinguish different classes of networks. The data used here come from the financial and oncology domains.

Fig.3 shows the Maxwell-Boltzmann entropy for the NYSE times series data. The figure is annotated to indicate the positions of significant financial events such as Black Monday, Friday the 13th mini-crash, Early 1990s Recession, 1997 Asian Crisis, 9.11 Attacks, Downturn of 2002-2003, 2007 Financial Crisis, the Bankruptcy of Lehman Brothers and the European Debt Crisis. In each case, the entropy undergoes significant fluctuation associated with dramatic changes in network structure.

A good example is the downturn of 2002-2003. After the 9.11 attacks, investors became nervous about the prospect of terrorism affecting the United States economy. Following the subsequent collapse of many internet companies, numerous large corporations were forced to restate earnings and investor confidence suffered. This considerably altered the interrelationships among stocks and resulted in significant variance in the structure of the entire market.

Next we explore whether the Maxwell-Boltzmann entropy can distinguish the tumor mutation networks for different types of cancers, i.e. the three major cancers cataloged in somatic mutation genes in Data set 3, which contains data for 356 ovarian cancer patients, 248 uterine cancer patients and 381 lung adenocarcinoma patients.

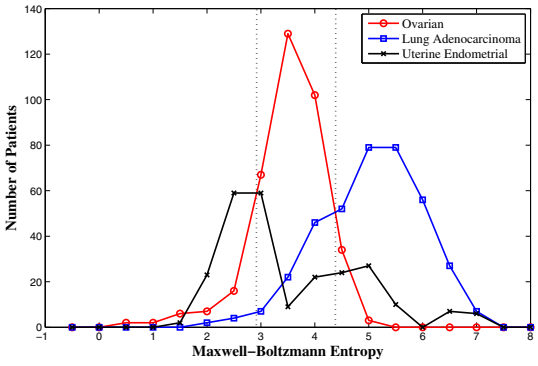

Figure 7. Histogram of Maxwell-Boltzmann entropy ($\beta = 10$) for three classes of tumor mutation networks (ovarian, uterine and lung adenocarcinoma).

In Fig.7, it shows the histogram of the Maxwell-Boltzmann entropy, together with the thresholds used to separate the three classes. The three different types of tumor networks span different entropy intervals, and can be separated using two entropy thresholds. The uterine and ovarian classes are best separated by an entropy threshold 2.92, which gives classification accuracies 33.87% and 83.71% for the two classes respectively. The ovarian and lung adenocarcinoma classes can similarly be best separated using an entropy threshold of 4.38, which gives classification accuracies of 83.71% and 78.48% respectively.

Here we conduct an exhaustive search for the two thresholds, with the objective of maximising the aggregate classification accuracy. This result empirically implies that although there exists a potential improvement in classification accuracy, the Maxwell-Boltzmann entropy can provide a useful unary feature for class separation.

Overall, the Maxwell-Boltzmann entropy resulting from classical energy level occupation statistics is able to reflect the structural properties of different networks. It also gives a better performance in distinguishing different network structures. This observation confirms that the thermodynamic characterization, especially entropy, is not only effective in the financial domain, but also provides some useful insights to analyze oncological data.

3.4. Evaluation

Now we compare the performance of the Maxwell-Boltzmann to the von Neumann entropies for a number of classification problems. We perform this analysis for both synthetic graphs i.e. the three models of complex networks (Erdős-Rényi random graphs, smalll-world networks and scale-free networks), and the cancer mutation data. Both data-sets are challenging since their overlap distribution of entropy for the different classes of graphs.

Because the classes in the data are severely in terms of the entropy, our approach applies the discriminant analysis classifier for the entropy to extract clusters, and then by identifying the modal cluster for each group and computing the classification accuracy. Table 1 and Table 2 summarize the results obtained using the Maxell-Boltzmann and von-Neumann entropies. For the synthetic graphs data the Maxwell-Boltzmann entropy outperforms the von-Neumann entropy on all classes of data presented by a margin of about 30%. In the cancer mutation data, the Maxwell-Boltzmann entropy performs best, except for the uterine cancer class.

Figure 4 compares the Maxwell-Boltzmann and von Neumann entropies for the financial time series data. Here the Maxwell-Boltzmann entropy reveals more fine structure in the times series. For instance, the early 1990s recession, the 1997 Asian crisis, the 9.11 attacks, the downturn of 2002-2003 and the 2007 financial crisis are all revealed by the Maxwell-Boltzmann entropy but not by the von Neumann entropy.

Another important parameter to discuss is the temperature. Low and high temperature will cause different situation in entropic representation. To evaluate the temperature effect on the financial data, we increase or decrease temperature leaving the number of particle unchanged. Fig.5 and Fig. 6 compare the high ($\beta = 0.2$) and low ($\beta = 20$) temperature situation in NYSE. As shown in the figures, both entropies in high and low temperature do not performance well in characterizing

Preprint submitted to 23rd International Conference on Pattern Recognition.
Received April 19, 2016.

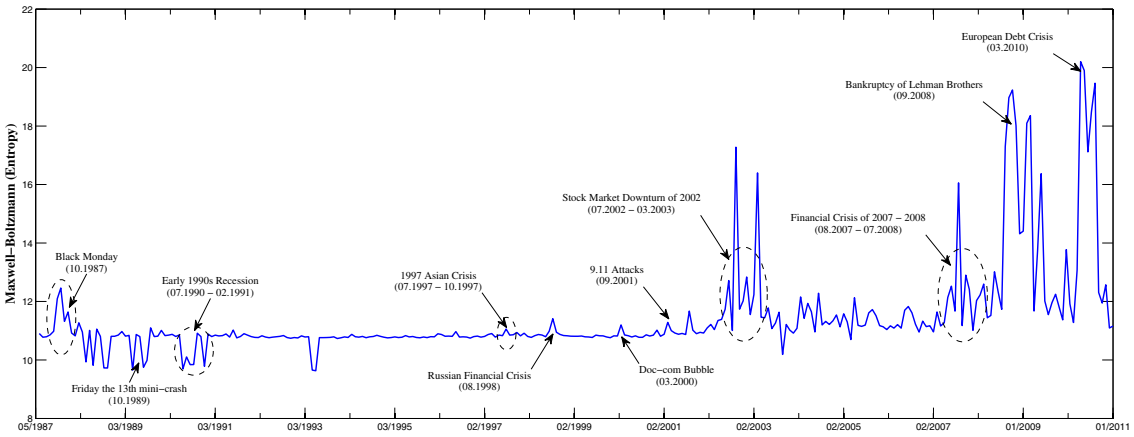

Figure 3. Maxwell-Boltzmann entropy for NYSE (1987-2011). Particle number $N = 5$, and temperature $\beta = 7$. Critical financial events, i.e., Black Monday, Friday the 13th mini-crash, Early 1990s Recession, 1997 Asian Crisis, 9.11 Attacks, Downturn of 2002-2003, 2007 Financial Crisis, the Bankruptcy of Lehman Brothers and the European Debt Crisis, all appear as distinct events.

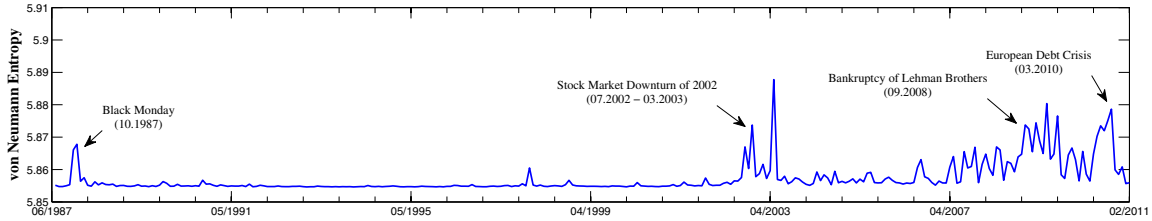

Figure 4. von Neumann entropy for NYSE (1987-2011). Although it can indicate a few critical financial events, there are some missing information, such as Friday the 13th mini-crash, Early 1990s Recession, 1997 Asian Crisis, 9.11 Attacks, Downturn of 2002-2003, 2007 Financial Crisis.

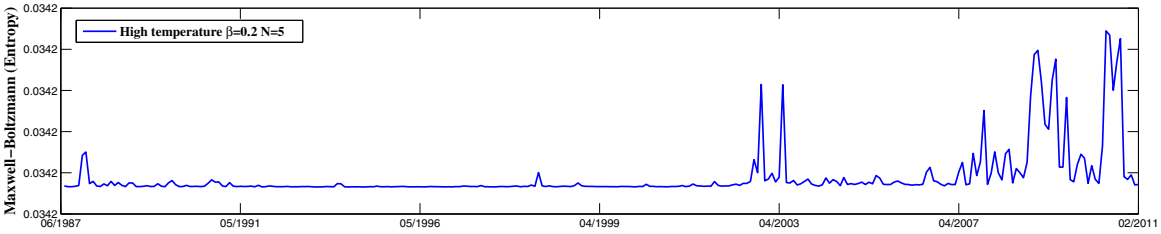

Figure 5. The high temperature situation in Maxwell-Boltzmann entropy for NYSE. Particle number $N = 5$, and temperature $\beta = 0.2$. Similar to the von Neumann entropy, which reduces the performance to identify critical financial events.

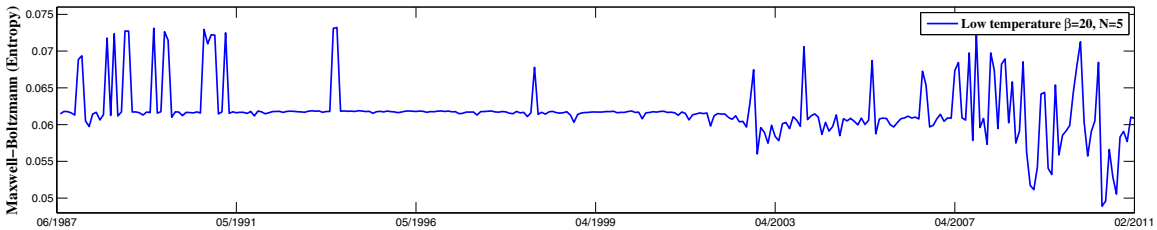

Figure 6. The low temperature situation in Maxwell-Boltzmann entropy for NYSE. Particle number $N = 5$, and temperature $\beta = 20$. It is difficult to indicate financial events.

Preprint submitted to 23rd International Conference on Pattern Recognition.
Received April 19, 2016.

TABLE 1. COMPARISON OF CLASSIFICATION ACCURACY FOR THREE SYNTHETIC NETWORK MODELS WITH ENTROPY FROM MAXWELL-BOLTZMANN STATISTICS AND VON-NEUMANN ENTROPY (PARTICLE NUMBER $N = 1$, TEMPERATURE $\beta = 10$)

Classification Accuracy	Random Graphs	Scale Free Networks	Small World Networks
Maxwell-Boltzmann Statistics	100% (30/30)	83.33% (25/30)	83.33% (25/30)
von-Neumann Entropy	60.00% (18/30)	56.67% (17/30)	66.67% (20/30)

TABLE 2. COMPARISON OF CLASSIFICATION ACCURACY FOR TUMOR NETWORKS WITH ENTROPY FROM MAXWELL-BOLTZMANN STATISTICS AND VON-NEUMANN ENTROPY (PARTICLE NUMBER $N = 1$, TEMPERATURE $\beta = 10$)

Classification Accuracy	Uterine Cancer	Ovarian Cancer	Lung Adenocarcinoma
Maxwell-Boltzmann Statistics	33.87% (84/248)	83.71% (312/372)	78.48% (300/381)
von-Neumann Entropy	56.85% (141/248)	69.89% (260/372)	64.83% (247/381)

network structure. The high temperature is similar to von-Neumann entropy, which leads to the distinction so small that many important financial events are disappearing. The low temperature causes the unstable variance in entropy, which is difficult to identify critical events. The same phenomenon is observed in synthetic and real-world tumor networks. As shown in Fig.8, both high and low temperature cases reduce the classification accuracy in network structure distinction.

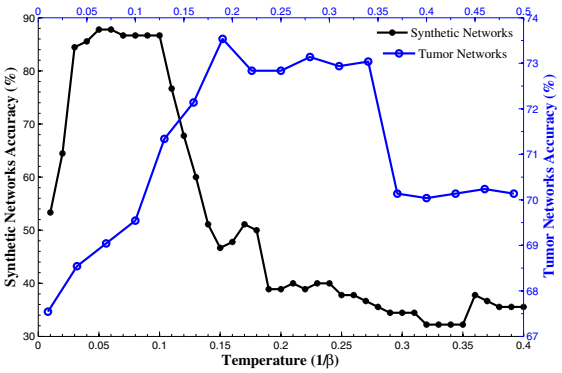

Figure 8. The classification accuracy of Maxwell-Boltzmann entropy changes with temperature for synthetic networks and real-world tumor mutation networks.

4. Conclusion

This paper explores the thermodynamic characterizations of a network resulting from the Maxwell-Boltzmann partition function, and specifically associated with the thermalisation effects of heat bath on the energy level occupation statistics. We have viewed the normalized Laplacian matrix as the Hamiltonian operator of the network with associated energy states which can be occupied by a system with distinguishable particles. We compute the thermodynamic entropy when the particle system is in thermodynamic equilibrium with a heat bath, and the energy states are occupied according to the Maxwell-Boltzmann distribution. We evaluate the resulting entropy as a tool for distinguishing different types of network structures in both static and time series data. These experiments demonstrate that thermodynamic entropy can be used to characterize the changes of network structure with time, and distinguish different types of network models (Erdős-Rényi random graphs, small world networks, and scale free networks). Future work will focus on exploring non-classical alternatives to the Maxwell-Boltzmann occupation statistics. These include Bose-Einstein and Fermi-Dirac statistics, which apply to systems of indistinguishable bosons and fermions.

References

[1] E. Estrada and N. Hatano, *Communicability in Complex Networks*, Physical Review E, 77, 2008.

[2] R. Albert and A. L. Barabasi, *Statistical Mechanics of Complex Networks*, Review Moden Physics, 74, 2002.

[3] J. Park and M. Newman, *Statistical mechanics of networks*, Physical Review E, 70(6), 2004.

[4] G. Bianconi, C. Rahmede and Z. Wu, *Complex Quantum Network Geometries: Evolution and Phase Transitions*, arXiv:1503.04739v2, 2015.

[5] D. Watts and S. Strogatz, *Collective dynamics of small world networks*, Nature, 393, 1998.

[6] C. Ye, R. C. Wilson, C. H. Comin, L. F. Costa and E.R. Hancock, *Thermodynamic Characterization of Networks Using Graph Polynomials*, Physical Review E, 92, 2015.

[7] K. Anand and G. Bianconi and S. Severini, *Shannon and von Neumann entropy of random networks with heterogeneous expected degree*, Physical Review E, 83(3), 2011.

[8] Mikulecky, *Network thermodynamics and complexity: a transition to relational systems theory*, Computers & Chemistry, 25, 2001.

[9] F. Passerini and S. Severini, *The von Neumann entropy of networks*, International Journal of Agent Technologies and Systems, 2008.

[10] F. Chung, *Spectral Graph Theory*, CBMS Regional Conference Series in Mathematics, 92, 1997.

[11] L. Han, E. Hancock and R. Wilson, *Characterizing Graphs Using Approximate von Neumann Entropy*, Pattern Recognition Letter, 33, 2012.

[12] C. Ye, R. C. Wilson, C. H. Comin, L. F. Costa and E.R. Hancock, *Approximate von Neumann entropy for directed graphs*, Physical Review E, 89, 2014.

[13] K.Huang, *Statistical Mechanics*, New York: Wiley, 1987.

[14] A. Barabasi and R. Albert, *Emergence of scaling in random networks*, Science, 286, 1999

[15] F. N. Silva, C. H. Comin, T. K. DM. Peron, F. A. Rodrigues, C. Ye, R. C. Wilson, E. Hancock, L.da F. Costa, *Modular Dynamics of Financial Market Networks*, Physics and Society, 2015

[16] The International Cancer Genome Consortium, *International network of cancer genome projects*, Nature, 464, 2010

[17] E.G. Cerami, B.E. Gross, E. Demir, I. Rodchenkov, O. Babur, N. Anwar, N. Schultzand, G.D. Bader, C. Sander, *Pathway Commons, a web resource for biological pathway data*, Nucleic Acids Res, 39, 2011

[18] M. Hofree, J. P. Shen, H. Carter, A. Gross, T. Ideker, *Network-based stratification of tumor mutations*, Nature Methods, 10, 2013

Preprint submitted to 23rd International Conference on Pattern Recognition.
Received April 19, 2016.